

## Article

# Modeling Non-Point Source Nutrient Loads with Different Cropping Systems in an Agricultural Lake Watershed in Southwestern China: From Field to Watershed Scale

Jiayu Peng <sup>1,2,†</sup>, Chunling Jin <sup>1,2,3,†</sup>, Yue Wu <sup>1,2,4</sup>, Zeying Hou <sup>1,2</sup>, Sijia Gao <sup>1,2</sup>, Zhaosheng Chu <sup>1,2,\*</sup> and Binghui Zheng <sup>1,2,\*</sup> 

- <sup>1</sup> National Engineering Laboratory for Lake Pollution Control and Ecological Restoration, Chinese Research Academy of Environmental Sciences, Beijing 100012, China  
<sup>2</sup> State Environmental Protection Key Laboratory for Lake Pollution Control, Chinese Research Academy of Environmental Sciences, Beijing 100012, China  
<sup>3</sup> Center for Water and Ecology, School of Environment, Tsinghua University, Beijing 100084, China  
<sup>4</sup> Engineering Research Center of Ministry of Education on Groundwater Pollution Control and Remediation, College of Water Sciences, Beijing Normal University, Beijing 100875, China  
\* Correspondence: chuza@craes.org.cn (Z.C.); zhengbinghui@craes.org.cn (B.Z.)  
† These authors contributed equally to this work.



**Citation:** Peng, J.; Jin, C.; Wu, Y.; Hou, Z.; Gao, S.; Chu, Z.; Zheng, B. Modeling Non-Point Source Nutrient Loads with Different Cropping Systems in an Agricultural Lake Watershed in Southwestern China: From Field to Watershed Scale. *Mathematics* **2022**, *10*, 4047. <https://doi.org/10.3390/math10214047>

Academic Editors: Fei Qi, Chao Liu and Yiping Wang

Received: 17 August 2022

Accepted: 28 October 2022

Published: 31 October 2022

**Publisher's Note:** MDPI stays neutral with regard to jurisdictional claims in published maps and institutional affiliations.



**Copyright:** © 2022 by the authors. Licensee MDPI, Basel, Switzerland. This article is an open access article distributed under the terms and conditions of the Creative Commons Attribution (CC BY) license (<https://creativecommons.org/licenses/by/4.0/>).

**Abstract:** Understanding the influence of cropping systems on non-point source pollution (NPSP) is crucial, since NPSP has become the major nutrient source of lake eutrophication. How to identify the characteristics of the N and P balance at different spatial and temporal scales remains a challenge in pollution control and decision-making. In this study, we built a soil and water assessment tool (SWAT) model coupled with an export coefficient model for a NPSP simulation in the North of Erhai Lake Basin (NELB). A method was proposed to study the N and P transport from fields and the individual sub-basins to Erhai Lake using SWAT simulation. The results showed that the N and P loss fields were mainly situated in the vicinity of the Fengyu river and along the mainstream of the Miju and Mici rivers. N and P loss fields were mainly occupied by rice–broad bean/rice–rapeseed crops and vegetables. While the critical N and P load contribution areas were situated in the vicinity of downstream of the Miju, Yong’an, and Luoshi rivers. The effects of different cropping systems on the N and P export to the watershed were insignificant in the NELB and decreased by 4–9% when changing cropping system compared to the original crops. The NPSP discharged from the critical areas was retained and purified by the flow and the reservoirs scattered along the rivers, and it was noticed that the N and P loss was mainly from the critical pollution discharge areas located downstream of Miju river. This study can provide an important simulation method for understanding NPSPs and, therefore, can help authorities improve agricultural land use and reduce lake pollution.

**Keywords:** NPSP; cropping system; N and P balance; pollution; SWAT; Erhai Lake

**MSC:** 03C98

## 1. Introduction

Lakes are very important ecosystems, providing drinking water resources, shipping, flood control, irrigation, aquaculture, tourism, and other functions [1]. However, lake eutrophication has become a challenging global environmental issue [2]. Excessive loading of nutrients (primarily phosphorus and nitrogen) from anthropogenic sources is a major cause of water quality impairment and lake eutrophication [3,4]. With the development of wastewater treatment facilities, the influence of point-source pollution in the watershed was diminished [5], but nutrients transported into water bodies from non-point source pollution (NPSP), including agricultural non-point sources, rural domestic wastewater, and urban and rural storm water, began to comprise a larger proportion [6–8]. Agricultural

non-point source pollution (ANPS) is of particular concern [9], contributing up to 50% of total nitrogen (TN) and total phosphorus (TP) in China; it is a major reason for the eutrophication of streams and lakes [10].

ANPS is challenging to trace and control due to its random and intermittent occurrence and the complicated mechanisms and processes that underlie it [11]. Quantifying agricultural nitrogen (N) and phosphorus (P) losses and elucidating their major pathways is essential to accurately estimate the environmental risks posed by ANPS pollution and for formulating appropriate control strategies [12].

Field monitoring methods can provide accurate NPSP load estimates. However, they are time-, money-, and labor-consuming, which usually results in a scarcity of monitored data, making these methods ineffective and limited at large scale. Mechanistic models have been widely used to simulate watershed/field scale hydrological processes [13] and the N and P circulation in various environmental compartments, including the atmosphere and surface water–vadose zone–groundwater system [14]. Therefore, modeling helps give a better understanding of the migration and transformation of pollutants in the real world [15]. Various models were used in the NPSP study, which developed from lump to spatially distributed models or from conceptual to numerical models. The classic conceptual models are the (P)USLE model and the Export Coefficient Model (ECM), which are simple to operate and have a reasonable accuracy [16]. SPARROW is a model between the numerical and conceptual models, but it is not considered a suitable option for NPSP simulation in small-scale watersheds [17]. The most widely applied numerical models include WEPP, soil and water assessment tool (SWAT), and HSPF, etc. [14]. Taking SWAT as an example, it can continuously simulate hydrologic and nutrient processes via a range of sophisticated modules (e.g., irrigation, fertilization, tillage, planting, impoundment, and drainage) [18]. SWAT has been utilized and verified in many NPSP studies in various watersheds [19–21].

In previous studies, the impacts of land use change on NPSP generation and discharge have received attention in SWAT simulations. Li et al. explained the contribution of land use type to the nitrogen export to Erhai Lake through SWAT simulation [22]. Zhang et al. pointed out that cropland had the highest contribution rate to TN and TP in the Three Gorges Reservoir Area [23]. However, change of land use is usually not very influential regarding nutrient loads, especially regarding agricultural land use. By contrast, when the cropping system is changed, which implies a different plant structure and fertilizer application and utilization, the N and P losses are altered at field scale [24]. However, few studies have focused on the evaluation of the N and P balance at field scale, or the estimation of the sub-basin N and P loads exported to the watershed, due to scarce data and the lack of a method to use SWAT simulation results.

Erhai Lake, located in Yunnan province, southwest China, is a typical plateau lake, with a long hydrological residential time. The warm temperature and abundant sunlight are favorable for the growth of algae [25]. With the fast development of the watershed, and intensive human activities generating excessive pollution loads to the lake, Erhai Lake has undergone eutrophication in recent years [26]. Erhai Lake Basin is a typical agricultural lake basin; it has been reported that the pollution resulting from agriculture and rural households represents more than 60% of the total pollution loads [27]. The cropping systems are also undergoing dramatic regulation in Erhai Lake Basin, especially since the local government abandoned the garlic plant, and chemical fertilizer has gradually been replaced by organic fertilizer [28]. After the implementation of these NPSP control measures, the influence of changes in the cropping systems on the NPSP nutrient loads in the basin urgently needs to be understood, to assess the risks and support the protection of Erhai Lake.

In this study, the SWAT model was applied to simulate NPSP loads in the North of Erhai Lake Basin (NELB). The three major objectives were: (1) propose a method to calculate N and P balance at the field scale and apply it in NELB; (2) propose a method to calculate the N and P export intensity at the watershed scale and apply it in NELB; and (3) examine

the effects of different cropping systems on the N and P export using scenario analysis. The results are expected to provide a scientific tool for NPSP control measure evaluation and implementation.

## 2. Materials and Methods

### 2.1. Watershed Description and Data Availability

NELB is located to the north of Erhai Lake Basin (ELB), Yunnan province, southwest China (Figure 1). The watershed area is 1222 km<sup>2</sup>, occupying 47.6% of ELB. The watershed has a plateau monsoon climate, with a mean annual temperature of 14.2 °C and annual rainfall of 744.9 mm [29]. The rainfall is distributed unevenly during the year, with more than 85% of rainfall occurring in summer and autumn, which favors the occurrence of non-point source pollution [8].

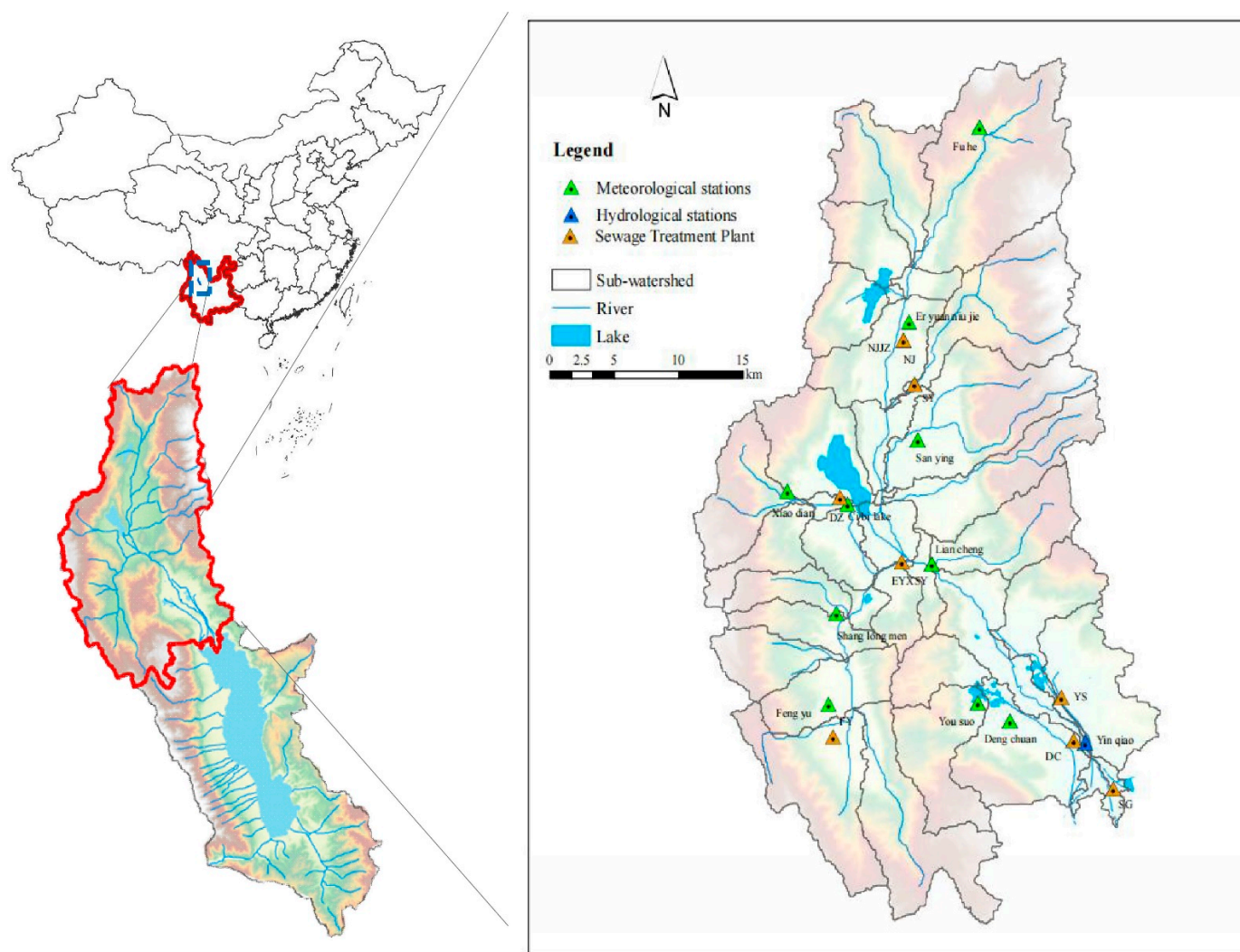


**Figure 1.** The location of NELB in the watershed.

The administrative region of NELB includes seven villages and towns in Eryuan county and one county in Dali City [30]. The northern region is the major water source for Erhai Lake, providing more than 50% of the inflow into the lake, which comes from Yong'an River, Miju River, Xizha River, and Luoshi River [31].

In the NELB region, the main land use type was forest (occupying 51.06% of the study area), followed by farmland (31.56%). Farmlands with intensive human activities including livestock and agriculture can be a major pollution source and rapidly transport

land pollutants (including N and P) to Erhai Lake [32]. The highest export of ANPS has been reported in the NELB region [33]. In the ELB, the water quality is inferior in the north of Erhai Lake compared to the middle and south.

The major farmland types were classified as paddy land, dryland, and orchards, which occupied 11.94%, 11.61%, and 2.28%, respectively, of the NELB. The major agricultural production types include rice–broad bean/rice–garlic (R–B/R–G), rice–broad bean/rice–rapeseed (R–B/R–R), vegetables (Vegeta.), and corn–broad bean/corn–rapeseed (C–B/C–G) (Figure S1). The plant types varied in different parts of the agricultural land and in different periods, according to the lunar calendar. In paddy soils, the rotation system is rice from May to September, then broad bean, rapeseed, or garlic in the other months. A typical dryland crop rotation includes corn (from May to September) alternating with broad beans and rapeseed (from October to April the following year). In recent years, the cropping system in Erhai Lake Basin has changed substantially, with a remarkable drop in the garlic-sown area, and the fertilizer type has shifted from mineral to organic.

The model inputs were divided into geography, meteorological, hydrological, water quality, pollution source, and water resource utilization data. A detailed data description and sources are shown in Table 1. SWAT was set up using digital elevation model (DEM), land use map, and soil map. Four years of daily precipitation from nine monitoring stations within the watershed, and the China Meteorological Assimilation Driving Datasets (CMADS) were combined to drive the hydrology and nutrient transport routines in SWAT. The hydrological station Yinqiao, located at the Miju River outlet, was used for model calibration and validation (Figure 1).

**Table 1.** Data and sources used in this study.

No	Data	Scale	Source	Parameter	Usage
1	DEM	1:50,000	Geospatial data website [34]	Elevation, slope, etc.	
2	Soil	1:500,000	Soil Science Database [35]	Soil density, saturated hydraulic conductivity, soil organic matter content	Basic data requirement of SWAT
3	Land use map	1:100,000	Institute of environmental information science, Chinese Academy of Environmental Sciences	Radiation utilization rate, harvest index under optimal growth conditions, etc.	
4	Agricultural management	Yearly	Dali Agricultural Bureau, Dali statistical yearbook, Eryuan statistical yearbook, field investigation	Planting mode, fertilization type and amount, livestock and poultry breeding, irrigation schedule, rural population	NPSP and water consumption condition of SWAT
5	Sewage treatment facility	Monthly	Dali Housing and Urban Rural Development Bureau	Wastewater Treatment amount, TN and TP concentration in discharged water	PSP of SWAT
6	Water resource regulation	Monthly	Dali branch of Yunnan Province Hydrology Bureau	Water discharged amount in every month	Water regulation of SWAT
7	Reservoir and pool	Monthly	Yunnan water resources and Hydropower Survey, design and Research Institute	Storage, water surface	Water regulation of SWAT
8	Meteorology	Daily	China Meteorological data network [36] and Dali Hydrological Bureau	Daily rainfall, temperature and evaporation	Model Drive
9	Hydrology and water quality	Monthly	Dali Hydrological Bureau	Monthly runoff, total nitrogen and total phosphorus concentration, suspended sediment	Calibrate and validate model

2.2. Method

2.2.1. Methodology Framework

The SWAT model can explain hydrology and pollutant transportation processes well; however, the generation and discharge of different pollutants, as well as the irrigation and reservoir regulation behavior should be preprocessed to couple with the SWAT model.

The watershed pollution sources include point source pollution (PSP) and NPSP. The PSP contained urban domestic wastewater, industrial wastewater, and centralized treatment wastewater, which may also have come from NPSP. NPSP included the pollution from agricultural production, livestock and poultry breeding, rural domestic sources, and wastewater (excluding urban areas and industry). Some of the NPSP results were down-scaled from annual to daily for inputting into SWAT, and this was called the coupling process of SWAT and ECM.

Once the SWAT model was set up, the methods to calculate the N and P balance at the field scale and the individual sub-basin N and P export to the watershed were described in this study. The N and P balance and transport to the outlet of the watershed were estimated in NELB. Through a scenario analysis of SWAT, the effect of changing the cropping system on the pollution loads to Erhai Lake was evaluated. Figure 2 shows the overall workflow of this study.

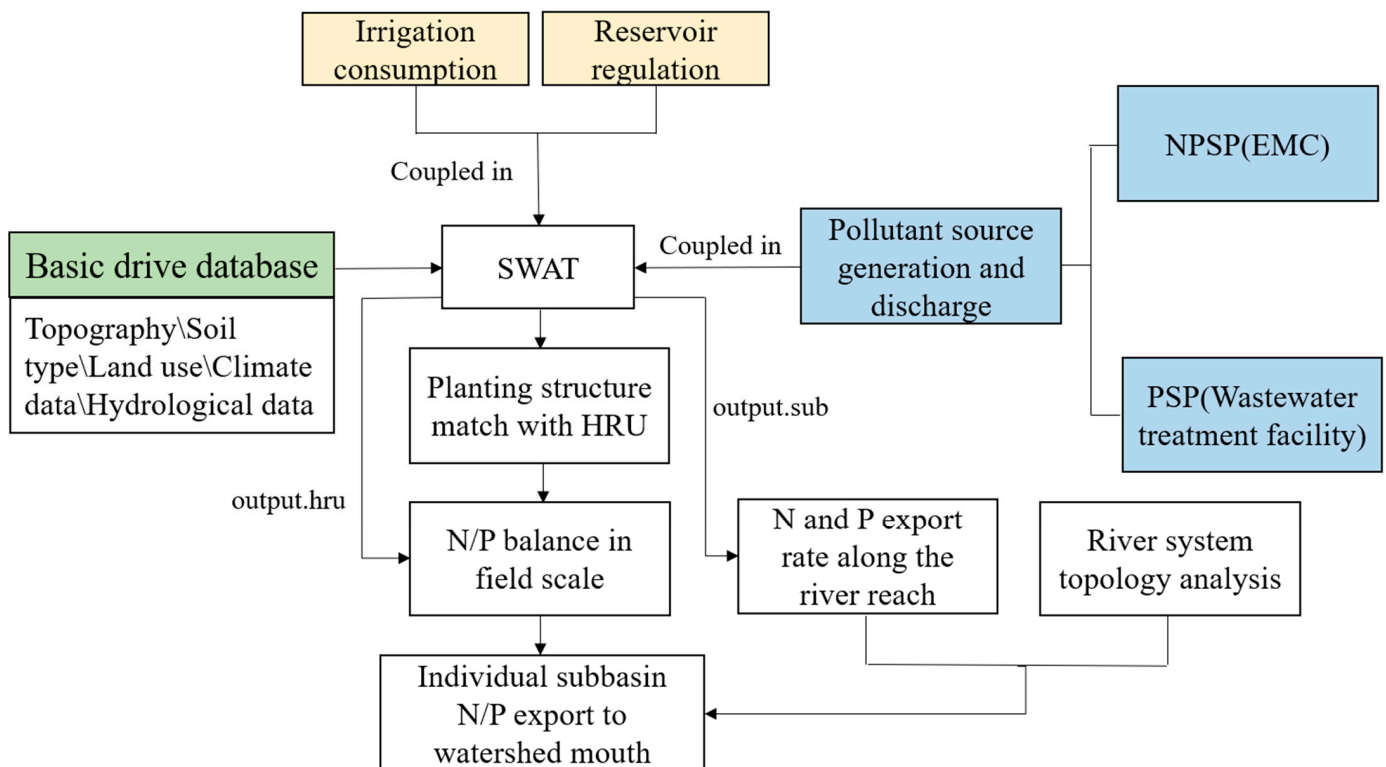


Figure 2. The overall workflow of the setting up of SWAT and its application in NELB.

2.2.2. SWAT Set Up

Pollution Source Input to SWAT

PSP

Urban domestic wastewater and industrial wastewater were discharged from the WWTP, and the flow and pollutant concentration data came from the records of the WWTP in the study area. The location of the WWTP is shown in Figure 1.

NPSP

The NPSP includes planting, livestock and poultry breeding, and village wastewater discharge.

(1) Planting

The fertilizer intensity and the application date of each crop were input into SWAT through the database named mgt. Detailed information about crop fertilization is shown in Table 2.

**Table 2.** Fertilizer management in NELB unit: kg/ha.

Crop Type	Fertilizer	Month/Day					
		4.1	5.1	6.1	10.1	11.15	1.1
Rice	N	56.06	22.425	33.63	0	0	0
	P	30.85	0	0	0	0	0
Corn	N	246.75	98.7	148.05	0	0	0
	P	79.81	0	0	0	0	0
Garlic	N	0	0	0	349.82	182.20	255.08
	P	0	0	0	98.68	0	0
Rapeseed	N	0	0	0	30.40	27.20	27.20
	P	0	0	0	47.70	11.30	11.30
Broad bean	N	0	0	0	53.00	56.90	56.90
	P	0	0	0	26.80	12.00	12.00

(2) Livestock and poultry breeding

The livestock and poultry breeding pollution loads were calculated using ECM, which was expressed as in Equation (1), with  $PI_{lp}$  used as a continuous input pollutant source in SWAT.

$$PI_{lp} = \frac{\sum_i^n N_i \times F_i}{A} \tag{1}$$

where  $PI_{lp}$  is the livestock and poultry breeding intensity, kg/ha per day;  $N_i$  is the number of  $i$  kind of livestock and poultry;  $F_i$  is the discharge parameter of  $i$  kind of livestock and poultry, kg/livestock and poultry, the discharge parameter of each livestock and poultry type can be seen in the Supplementary Materials; and  $A$  is the area of the sub-basin, ha.

(3) Rural domestic wastewater

Rural domestic wastewater discharge was calculated using ECM, which was estimated with Equation (2);  $PI_{rd}$  was used as a continuous input pollutant source in SWAT.

$$PI_{rd} = P * F_c / A \tag{2}$$

where  $PI_{rd}$  is the rural domestic wastewater discharge intensity, kg/ha per day;  $P$  is the size of rural population;  $F_c$  is the discharge parameter, kg/capita, the discharge parameter of the rural population can be seen in the Supplementary Materials; and  $A$  is the area of sub-basin, ha.

Water Resource Consumption and Regulation

The irrigation intake water of each sub-basin was estimated using the product of the crop area and its irrigation schedule (Table 3), and its input to the database was named the WUS of SWAT.

**Table 3.** The irrigation schedule of the different crops in Erhai Lake Basin unit:m<sup>3</sup>/ha.

Crop Type	Month											
	6	7	8	9	10	11	12	1	2	3	4	5
Corn	3.00	0.00	0.00	0.00	0.00	0.00	0.00	0.00	0.00	0.00	3.00	3.34
Rice	6.40	1.93	1.93	1.00	0.00	0.00	0.00	0.00	0.00	0.00	1.33	15.07
Broad bean	0.00	0.00	0.00	0.00	0.00	2.40	2.40	2.40	2.40	2.40	0.00	0.00
Rapeseed	0.00	0.00	0.00	0.00	0.00	3.00	3.00	3.00	3.00	2.00	0.00	0.00
Vegetable	0.00	0.00	0.00	0.00	0.67	2.00	2.00	3.00	3.00	3.00	2.00	2.00

The Cibihu reservoir is an important water control project in Eryuan County and receives the inflow from the Mici River and Fengyu River, flows into the Xier River, then flows into the Miju River (Table 4). For sub-basins 9 and 20, the water consumption was simulated every month for the simulation of the inflow of the Cibihu reservoir, and the reservoir outflow was generalized as a PSP to Miju River. Although the investigation data were only obtained in 2014 and 2015, the water regulation condition for the rest of the year was zoomed in and out at an equal scale of the flow of the Miju River.

**Table 4.** The inflow and outflow of Cibihu Reservoir (unit 10<sup>4</sup> m<sup>3</sup>/d).

Month		1	2	3	4	5	6	7	8	9	10	11	12
2014	Fengyu River	7.5	17.9	7.6	10.4	0.0	21.7	19.4	21.9	13.3	20.6	7.3	6.8
	Mici River	0.0	0.0	0.0	0.0	0.0	0.0	4.2	0.0	0.0	5.8	0.0	0.0
	Reservoir Outflow	4.9	17.9	5.1	10.2	38.5	25.9	21.6	21.6	7.4	2.0	0.0	0.1
2015	Fengyu River	6.0	8.0	10.4	5.7	0.0	15.0	21.9	30.6	59.6	33.8	16.5	0.0
	Mici River	0.0	0.0	0.0	0.0	0.0	0.0	0.0	0.0	0.0	21.9	0.0	0.0
	Reservoir Outflow	5.4	8.0	6.8	1.7	37.3	42.1	19.0	10.8	58.6	19.6	11.1	0.0

### Model Calibration and Validation

#### (1) Calibration and validation results

The hydrology and water quality monthly data at Yinqiao monitor station, outlet of the NELB, were chosen for calibration and validation of the model results. The data from 2013–2014 were used to calibrate SWAT, and data from 2015–2016 were used in the validation of the SWAT outputs. The Nash–Sutcliffe efficiency (NSE) and coefficient of determination (R<sup>2</sup>) were used to test the accuracy of the model. The four variables selected for calibration and validation were flow, sediment, TN, and TP, and the results are shown in Table 5.

**Table 5.** R<sup>2</sup> and NSE of the four variables used in calibration and validation.

Process	Variable	Flow (Q)	Sediment	TN	TP
Calibration	R <sup>2</sup>	0.84	0.57	0.59	0.55
	NSE	0.79	0.59	0.56	0.52
Validation	R <sup>2</sup>	0.80	0.52	0.53	0.52
	NSE	0.70	0.50	0.50	0.50

#### (2) Parameter sensitivity

The calibration process was conducted with SWAT-CUP using the SUFI-2 method, and the parameter regulation results are shown in Table 6.

**Table 6.** The parameters influencing the results during calibration.

Variables	Parameter	Definition	Modify	Value
Runoff	SOL_K(1)	Saturated hydraulic conductivity	r	1.2
	CN2	Initial SCS runoff curve number for moisture condition	r	0.8
	GW_DELAY	Groundwater delay time	v	200
	ALPHA_BF	Baseflow alpha factor	v	0.006
	SLSUBBSN	Average slope length	r	1.4
	ESCO	Soil evaporation compensation factor	v	0.95
	GWQMN	Threshold depth of water in the shallow aquifer required for return flow to occur	v	1
	CH_N2	Manning’s “n” value	v	0.04
	CH_K2	Effective hydraulic conductivity in main channel alluvium	v	2
	SURLAG	Surface runoff lag coefficient	v	5

Table 6. Cont.

Variables	Parameter	Definition	Modify	Value
Sediment	USLE_P	USLE equation support practice factor	r	0.0057
	SED_CON	Sediment concentration in runoff, after urban BMP is applied	v	3387.34
	SPCON	Linear parameter for calculating the maximum amount of sediment that can be re-entrained during channel sediment routing	v	0.000518
	SPEXP	Exponent parameter for calculating sediment re-entrained in channel sediment routing	v	1.583371
	CANMX	Maximum canopy storage	r	−0.31118
Water Quality	CDN	Denitrification exponential rate coefficient	v	1.437
	SDNCO	Denitrification threshold water content	v	0.547
	NPERCO	Nitrate percolation coefficient	v	0.215
	RSDCO	Residue decomposition coefficient	v	0.06136
	PPERCO	Phosphorus percolation coefficient	v	16.487
	PHOSKD	Phosphorus soil partitioning coefficient	v	199.10
	ERORGN	Organic N enrichment ratio for loading with sediment	v	0.005
	ERORGP	Phosphorus enrichment ratio for loading with sediment	v	0.465

r represents the relative percentage's original value for the parameter increase/decrease. v represents the original value of the parameter that was replaced by the modified value.

### 2.2.3. N and P load Balance at Field Scale

SWAT delineated the watershed of NELB as comprising 35 sub-watersheds and 268 hydrologic response units (HRUs). HRU is the smallest unit of the study area with a homogeneous underlying surface, and the corresponding crop type in an HRU is single. Then the N and P balance in HRU can be seen as the N and P balance at the field scale.

The N and P removal or utilization rate at field scale were calculated using the variables within HRU scale (Equations (3) and (4)).

$$R_{ij} = \frac{P_{out}}{P_{in}} \quad (3)$$

$$U_{ij} = 1 - R_{ij} \quad (4)$$

where  $R_{ij}$  is the N or P removal rate in the  $j$ -th (1–35) sub basin and  $i$  kind (2–13) of HRU, %;  $P_{out}$  is the N or P output load obtained from the sum of N or P input items (Nitrogen fertilizer applied, Phosphorus fertilizer applied, etc.) in output.hru file, kg;  $P_{in}$  is the N or P input load obtained from the sum of N or P output items (Plant uptake of nitrogen, Plant uptake of phosphorus, etc.) in output.hru file, kg;  $U_{ij}$  is the utilization rate of N or P in the  $j$ -th (1–35) sub-basin and  $i$  kind (2–13) of HRU, %.

### 2.2.4. N and P Export to the Watershed Outlet

Pollutants generated from the upstream sub-basins flowed directly to the connected downstream sub-basins and finally reached the watershed outlet, after a certain amount of transition (Figure 3). This hydrological process (also including most nutrient transport) can be explained by the cumulative effect of the river network [20,33], which indicated that the pollutants of all upstream watersheds would accumulate at the downstream outlet.

The transfer coefficient (R) of pollutants was calculated in the sub-basin based on the method proposed in reference [10,37]. The export of N and P loads within a sub-basin to the watershed outlet can be calculated using Equations (5) and (6):

$$SUB_{i\_export} = SUB_{i\_source} * R_i \quad (5)$$

$$R_i = \prod_{j=i}^n \frac{RCH_{j-out}}{RCH_{j-in}} \tag{6}$$

where  $SUB_{i-export}$  is the N or P flux of  $i$ -th sub-basin export to the watershed outlet, kg;  $SUB_{i-source}$  is the total amount of N or P in  $i$ -th sub-basin, kg;  $R_i$  is the transfer rate of N or P export from  $i$ -th sub-basin to the watershed outlet, %;  $RCH_{j-out}$  is the output of N or P of  $j$ -th reach, kg;  $RCH_{j-in}$  is the input of N or P of  $j$ -th reach, kg;  $n$  is the accumulative sub-basin number of  $j$ -th reach flows. All the above variables were obtained from the output.rch and output.sub files in SWAT.

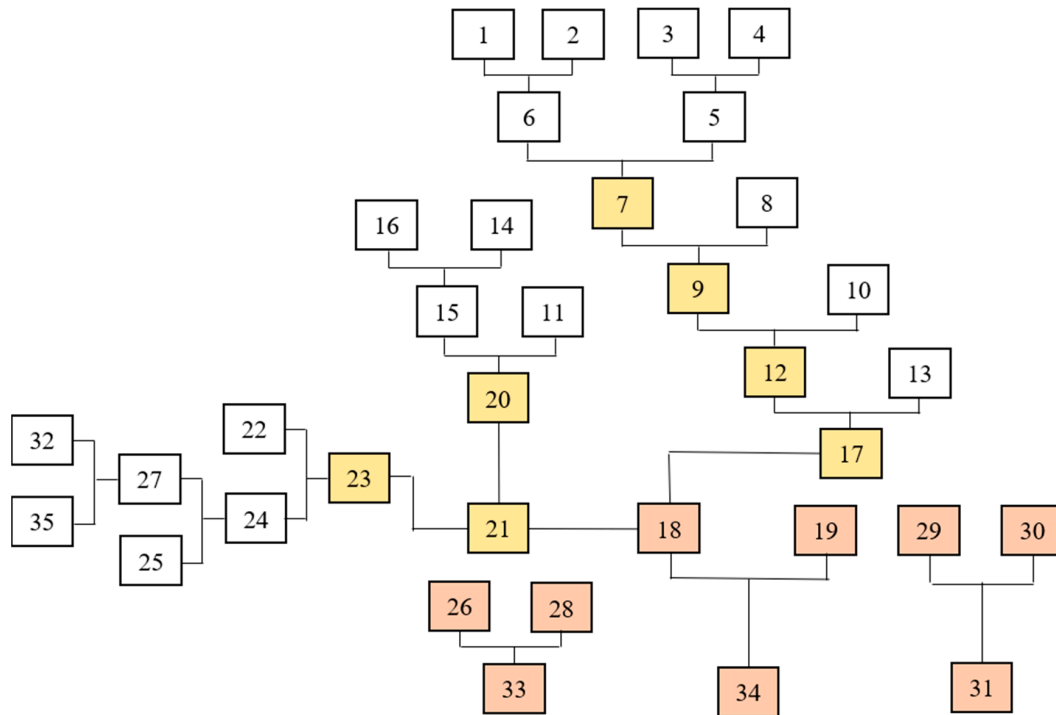


**Figure 3.** The topological relationship among the 35 sub-basins. The white boxes are upstream in the river water system, whereas those in yellow are in the middle parts, and those in red are downstream.

The topological relationship of 35 sub-basins is shown in Figure 3. It was found that the downstream of the North Three River is the Xiashankou section [38], which is located in sub-basin 18. Therefore, the sub-basins below 18 were categorized as downstream. The tributary originated from mountains defined as upstream, with an average slope of 13.71. The reaches between upstream and downstream were called the midstream, with an average slope of 9.22.

### 2.2.5. Influence Analysis on Cropping System Shifts

Once the SWAT model of NELB was built, the influence of changes in the cropping system on N and P export loads could be simulated. The business-as-usual (BAU) scenario was that the cropping system was maintained in its original state, and the other scenario (S) was the altered cropping system, in which garlic production system was not allowed during the simulation periods. Simulation of two scenarios was achieved by changing the fertilizer input data (Table 2) in the mgt file of SWAT. Then, the difference in N and P loads exported before and after the cropping system change could be compared.

## 3. Results

### 3.1. N and P Balance at Field Scale

The main agricultural systems in the NELB were classified as Vegeta., R-B/R-G, R-B/R-R, and C-B/C-R. The N and P balances at the field scale are shown in Figure 4.

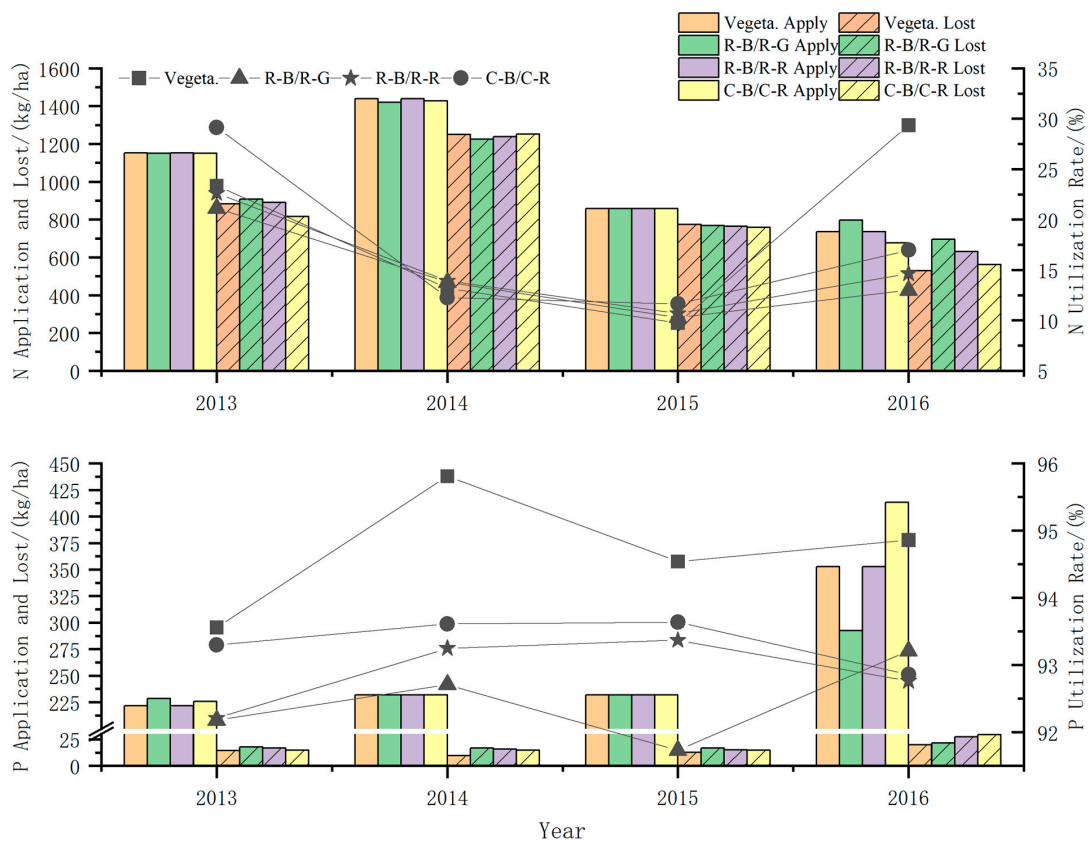


**Figure 4.** N and P input and utilization in different cropping systems from 2013 to 2016.

(1) N and P application rates

The average N application were 1150.71, 1431.12, 857.22, and 736.10 kg/ha in Vegeta., R-B/R-G, R-B/R-R, and C-B/C-R, respectively. In the four years considered, there was initially a rising trend, followed by a downtrend. In the same agricultural systems, the average P applications were 224.22, 231.76, 231.76, and 352.88 kg/ha, respectively, all with a gradually rising trend.

(2) N and P losses

The average N loss were 873.89, 1240.62, 766.10, and 603.75 kg/ha in Vegeta., R-B/R-G, R-B/R-R, and C-B/C-R, respectively, with proportionally similar losses in different cropping systems. In the same systems, the average P loss was 15.95, 14.26, 14.81, and 24.50 kg/ha, respectively, with a declining and then a rising trend.

(3) N and P balance

The average annual N balance was 276.83, 190.50, 91.11, and 132.35 kg/ha in Vegeta., R-B/R-G, R-B/R-R, and C-B/C-R, respectively. The N utilization rate in these four cropping systems was 24%, 13%, 11%, and 18%, respectively, with a declining trend until 2015, and then an increase in 2016.

The average annual P balance was 208.27, 217.50, 216.95, and 328.38 kg/ha in Vegeta., R-B/R-G, R-B/R-R, and C-B/C-R, respectively. The P utilization rate in these four systems was 93%, 94%, 94%, and 93%, respectively. The P utilization rate in vegetable and R-B/R-G fields increased in 2014, then declined in 2015, and increased again in 2016, whereas the P utilization rate in R-B/R-R and C-B/C-R fields showed a rising trend before 2015, and then declined in 2016.

3.2. N and P Export Intensity to the Watershed

The N export intensity from individual sub-basins to the watershed outlet from 2013 to 2016 is shown in Figure 5. The average annual N export intensities to the watershed mouth were 1.005, 0.837, 0.537, and 0.649 kg/ha per year from 2013 to 2016, showing a declining trend. The N export intensity varied in the 35 sub-basins, with the maximum

N export intensity in the no. 18 sub-basin (11.224, 7.415, 4.928, and 5.398 kg/ha per year in the four consecutive years), and the second was no. 34 (2.246 to 3.320 kg/ha per year during the study periods). Sub-basins 9, 7, 21, 23, and 26 also had a relatively high N export intensity. The sub-basins with the lowest N export intensity were 1, 3, 15, and 16, with a value of 0.001 kg/ha per year. These areas were usually the headwaters of the watershed, thus the long transport route was beneficial for the purification of N.

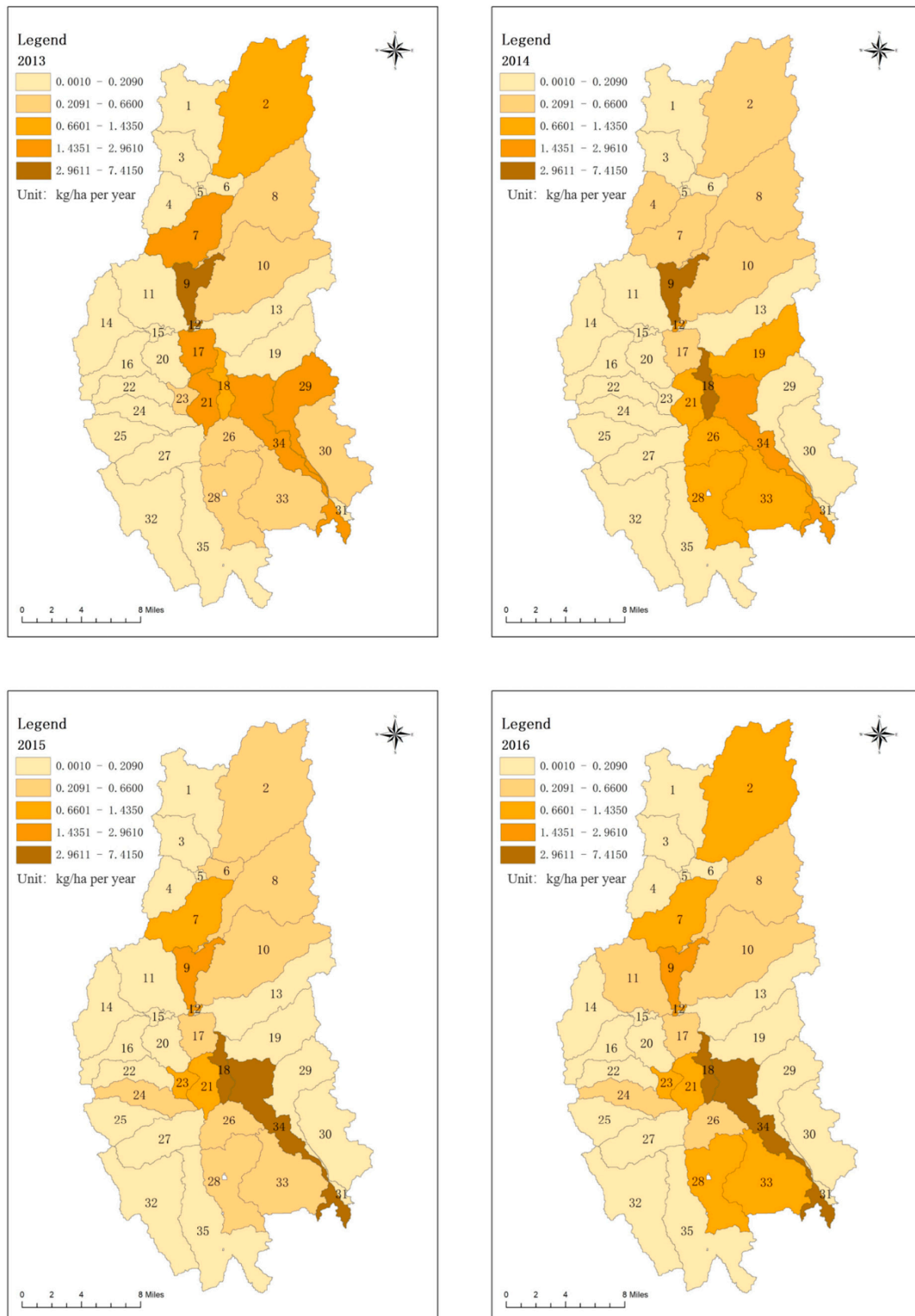


Figure 5. Sub-basin N export to Erhai Lake from 2013 to 2016.

The average annual sub-basin P export intensities to the watershed outlet were 0.231, 0.141, 0.146, and 0.124 kg/ha per year from 2013 to 2016, with a declining trend (Figure 6). The sub-basin with maximum P export intensity was no. 34, with values of 2.892, 1.674, 1.439, and 1.197 kg/ha per year from 2013 to 2016. The sub-basin with the second largest P export intensity was no. 18 (0.939, 0.634, 0.644, and 0.658 kg/ha per year from 2013 to 2016). The intensive P export areas were in the southwest, northeast, and downstream of the river basin, and the area reduced in size over the years.

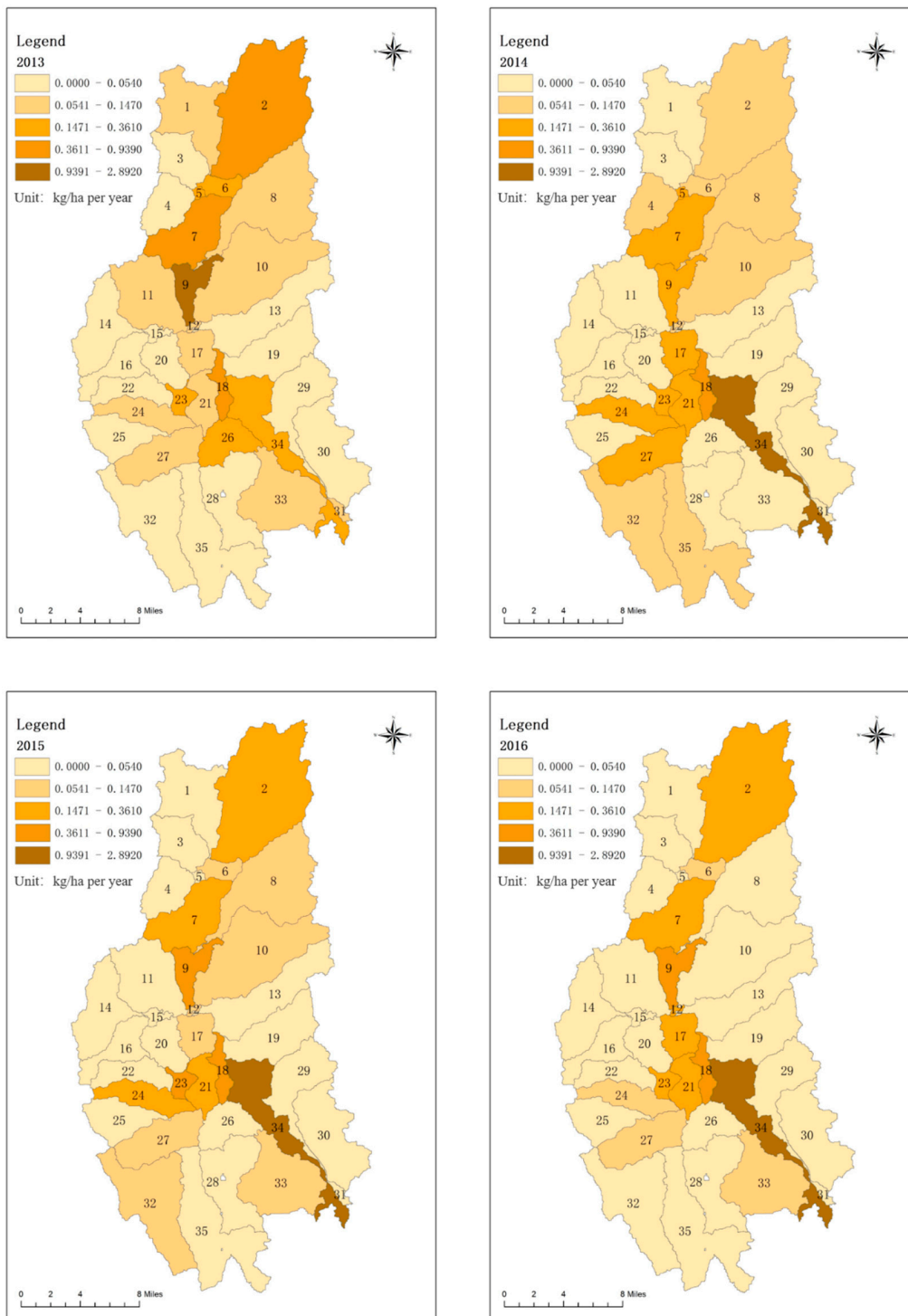


Figure 6. Sub-basin P export to Erhai Lake from 2013 to 2016.

### 3.3. N and P Load Change under Different Cropping Systems

The comparison of N and P loads under different cropping systems was analyzed using SWAT, and the results are shown in Figure 7. Under the BAU scenario, the N loads were 754.25, 687.16, 546.22, and 602.81 t from 2013 to 2016, and the P loads were 32.05, 16.81, 16.43, and 13.81 t in the same four consecutive years. After changing the cropping system, the N loads were 722.23, 670.24, 535.66, and 584.14 t, and the P loads were 30.68, 16.22, 15.12, and 12.61 t in the four consecutive years. Compared with the BAU scenario, the N load in S decreased by 4.25%, 2.46%, 1.93%, and 3.10%, and the P load in S decreased by 4.70%, 3.49%, 9.51%, and 8.81% in the four consecutive years.

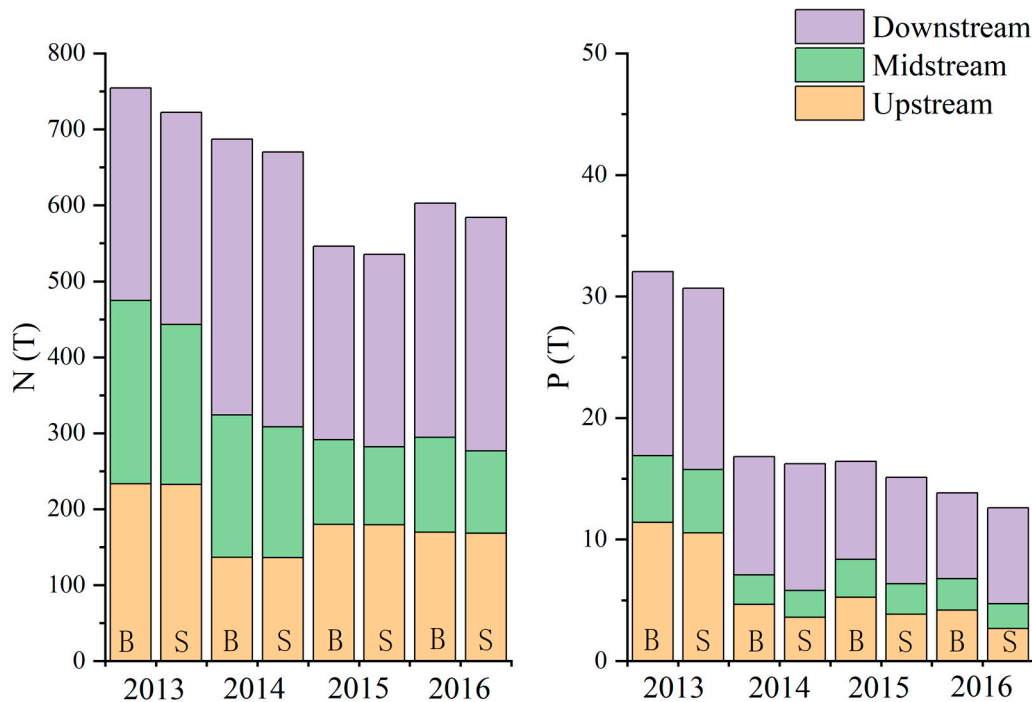


Figure 7. N and P load in different stream sections under varied cropping systems.

From the distribution of N and P loads, the average N loads from the upstream, midstream, and downstream areas were 179.82, 166.31, and 301.42 t, respectively, and the P loads from these three sections of the basin were 6.38, 3.40, and 10.00 t. The N discharge intensities were 0.25, 1.38, and 0.96 kg/ha per year, and the respective P discharge intensities were 0.09, 0.28, and 0.32 kg/ha per year.

When the cropping system was changed, the biggest change in N load appeared in the midstream area; compared to BAU, the N load decreased by 11%. A slight decrease of N loads occurred in the upstream and downstream areas, with a decrease of 0.4% and 0.3%, respectively. After the cropping system change, the biggest decrease in P load occurred upstream, with an annual decrease rate of 23.2%, whereas a 14% decrease in P load occurred midstream, and a 6.5% annual P load increase was noted downstream.

## 4. Discussion

### 4.1. Implications for Regional NPSP Management

Compared to BAU, the change of N and P loads at the outlet in NELB varied between 4 and 9% in the S1 scenario. The effects of changing the cropping system on the N and P loads into the lake were insignificant in the NELB. According to a previous study, livestock and poultry breeding were major sources of pollution, but planting was not a major pollution source in the NELB region [32,39]. The simulation indicated that the critical source areas were not critical load contribution areas [16]. The fields with the highest N and P loss

rates, R-B/R-R and vegetable fields, were mainly located in the Fengyu River Basin and along the mainstream (Figure S1). Meanwhile, there was a greater N and P export from the sub-basins that were closer to the watershed outlet [37]. It is shown in Figure 8 that seven sub-basins, which occupied only about 20% of the total watershed area, contributed approximately 60% of the total N loads. The export of P loads appeared more centralized, with sub-basins no. 34 and no. 2, contributing approximately 70% of the total P export. Moreover, these sub-basins were located midstream and downstream of the basin. These results indicated that the Fengyu River watershed (the sub-basin upstream of the No 23 sub-basin) was not the major contributor to the nutrient load of NELB., although it is the major NPSP generation and discharge area.

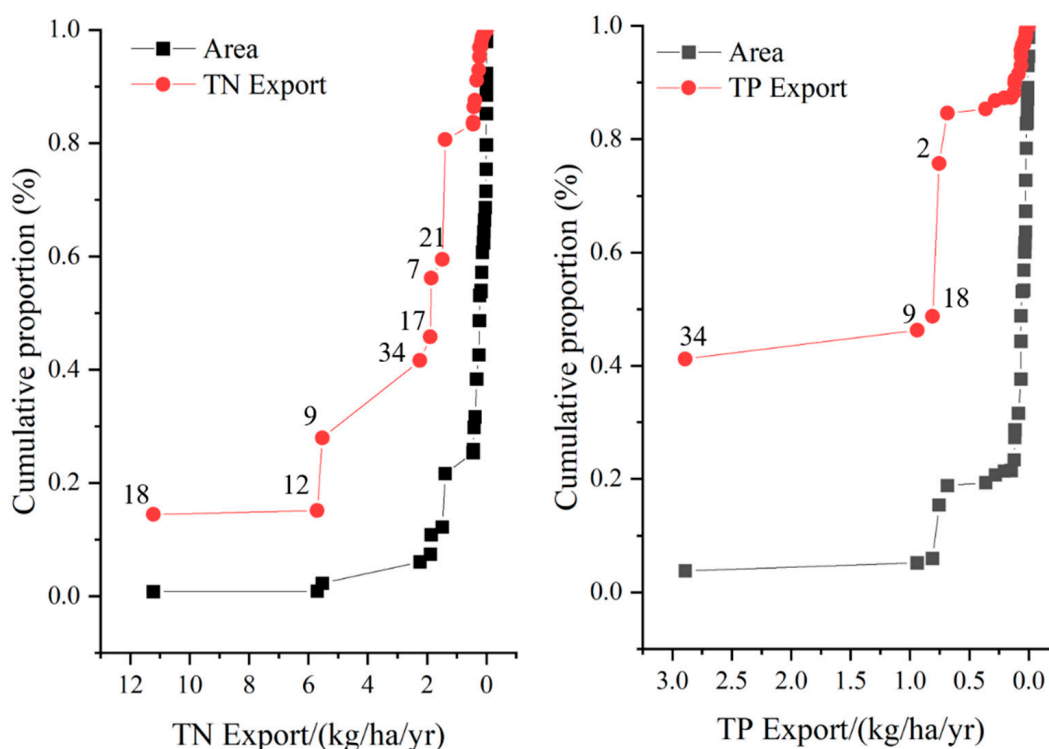


**Figure 8.** Contribution of individual sub-basins to the N and P export at the NELB outlet.

A past study reported that artificial wetland and impoundments would prolong the hydrological residence time, to enhance pollution purification [40]. Ponds and wetlands were scattered around the NELB; therefore, the pollutants from the tributary were purified along the river and it did not contribute the majority of nutrients to the watershed outlet. The mainstream and downstream were the major nutrient contributors in the NELB, due to the short distance from the mainstream outlet and the steeply inclined slope.

For more efficient NPSP control, the discharge of NPSP into the tributary should maintain its current state, and the intensity of human activities should be reduced in the mainstream. More wetlands or impoundments should be built, to enhance biological purification and phytoremediation.

#### 4.2. Implications for Erhai Lake Ecology Restoration

Erhai Lake is located at the headwater of the Yangtze River, and it is an important environmental and potable water resource. The ecological restoration of Erhai Lake is critical to the Yangtze River. However, Erhai Lake is a mesotrophic lake and undergoing fast social development, accelerating the eutrophication processes. Our research summarized the reference data on lake basin pollution export intensity along the Yangtze River (Table 7). The data indicated a gradually increasing trend of the N and P export intensity along the

Yangtze River. In terms of Erhai Lake, the N and P export intensities are relatively low under the stringent pollution control measures of this watershed compared to other lake basins, but the eutrophication of Erhai Lake is not under control. The trophic level index (TIL), the main indicator for assessing the degree of eutrophication of water bodies in China, taking into account the water body nutrient status obtained by chlorophyll a, TN, TP, COD<sub>Mn</sub>, transparency, etc., fluctuated around 40, which is between oligotrophic and eutrophic lakes ( $30 \leq \text{TIL} \leq 50$  indicates moderate eutrophication).

The stable equilibria theory indicates that once the status of a lake's ecological system has changed, it is challenging to return it to its original state. The clean and pollutant states of a lake water system can exist under the same nutrient loading [41]. Stability domains typically depend on slowly changing variables, such as land use, nutrient stocks, soil properties, and the biomass of long-lived organisms; however, these environmental factors are undergoing rapid change under the pressure of local socioeconomic development. In addition, stochastic events, such as hurricanes, droughts, and disease outbreaks, are usually difficult to predict and control, and it is easy to trigger a shift of state [42].

Therefore, the evidence showed that regarding the unstable state of the Erhai Lake water system, in order to hinder the deterioration of lake, it is better to restore the ecosystem than to damage it. Thus, pollution control measures, alone, are insufficient, and further ecological restoration measures are needed to restore Erhai Lake [43].

**Table 7.** Comparison of N and P export intensity in different lake watersheds.

Lake	N Export Intensity (kg/ha per Year)	P Export Intensity (kg/ha per Year)	Recharge Coefficient	TIL	Reference
Dianchi Lake	2.7	0.27	9.6	62.897	[44]
Erhai Lake	3.24	0.20	11.2	41.393	[39]
Fuxian Lake	3.77	0.34	4.5	24.870	[45]
Tai Lake	270	90	15	54.709	[46]
Chao Lake	280	12.1	12	54.287	[47]
Dongting Lake	26.05	1.60	55	48.176	[48]
Poyang Lake	2.33	0.11	105.7	47.600	[49]
Three Gorges Reservoir	3.917	0.277	110.7	51.740	[10,50]
North part of Erhai Lake basin (this study)	1.005	0.231	–	–	–

#### 4.3. Method Advantages and Limitation

Determining the N and P balance using N and P inputs and outputs is a common method and can identify the primary driving forces and provide a framework for measuring agroecosystem performance and environmental sustainability [51]. However, this common method (determining the N and P balance using N and P inputs and outputs) must be performed yearly and on administrative area scale. However, SWAT can simulate the nutrient balance and transportation on a more refined spatial and temporal scale [52].

SWAT coupled with ECM also improved the performance of the numerical model. It has been widely used to study pollution sources and transfer mechanisms [53]. This study proposed a method for N and P balance at the field scale utilizing the above-stated coupled model. It can identify the influence of cropping systems on NPSP at different spatial scales, which is beneficial for best management practices for the government. Moreover, this method has a wide application, especially in studying the interception and purification of different grades of rivers, wetlands, and lakes that are polluted with different nutrients or chemicals.

Considering its drawbacks, the SWAT model is not very applicable and advantageous in soil hydrological conditions [54], and it also does not simulate an aquifer's nitrate concentration correctly [55]. The measured data of the TN and TP flux from cropland via runoff to rivers and ditches contained uncertainties. In the current study, the TN and TP flux estimates were based on the hydrological and water quality tour gauging data,

performed three times per month. However, the TN and TP flux estimates were generally greater during the summer, because extreme events greatly influenced the nutrient flux. Approximately half of the annual TN and TP flux occurred on extreme days that accounted for less than 20% in the same year [56]. In addition, the SWAT model simplified the processes of several reservoirs in the NELB, due to a lack of investigation data, and this simplification in the model can increase the uncertainty level to some degree.

## 5. Conclusions

To characterize the influence of the changing cropping system on ANSP in the agricultural watershed north of Erhai Lake Basin, a SWAT model was built to simulate the pollutant transport processes. Based on the SWAT results, a method to estimate the N and P balances at the field scale and the N and P export intensities from individual sub-basins to the watershed outlet was proposed. The spatial and temporal changes in the N and P loads in the NELB with a change in the cropping system were discussed.

The N balance was largest in the vegetable fields, and the P balance was largest in the C-B/C-R cropping system. Around 20% of the watershed area contributed approximately 60% of the total N or P load, and the mid- and downstream sections in NELB were the major polluted areas. Changing the cropping system could decrease the sub-basin N and P loads to the outlet by 4–9%. The layout of dryland and paddies should be optimized; the mid- and downstream areas of the NELB should adopt more effective NPSP control measures, rather than just changing the cropping system.

This study proposed a method to estimate the N and P balances at the field scale and the sub-basin N and P export contributions to a watershed outlet, based on simulation using the SWAT model. This is beneficial for evaluating the influence of NPSP in data-scarce areas. However, the uncertainties of the SWAT model, either contained in the model simulation principle or arising from the accuracy of the data, should be addressed by improving the monitoring frequency and developing model functions. The effectiveness of NPSP control should be further improved by optimizing the fertilization rates and irrigation in the agroecological systems.

**Supplementary Materials:** The following supporting information can be downloaded at: <https://www.mdpi.com/article/10.3390/math10214047/s1>. Table S1: The discharged parameter of rural domestic life; Table S2: The livestock and poultry discharged parameter; Figure S1: The major planting structure in the North of Erhai Lake Basin.

**Author Contributions:** Writing—original draft, J.P., C.J., Z.H., Y.W. and S.G.; Writing—review and editing, Z.C. and B.Z. All authors have read and agreed to the published version of the manuscript.

**Funding:** This research was funded by the special fund of Chinese central government for basic scientific research operations in commonweal research institutes, the Chinese Research Academy of Environmental Sciences (2021KSKY-03).

**Conflicts of Interest:** The authors declare no conflict of interest.

## References

1. Qin, B. Lake eutrophication: Control countermeasures and recycling exploitation. *Ecol. Eng.* **2009**, *35*, 1569–1573. [[CrossRef](#)]
2. Jiao, J.; Tang, W. Dynamics of a lake-eutrophication model with nontransient/transient impulsive dredging and pulse inputting. *Adv. Differ. Equ.* **2021**, *2021*, 280. [[CrossRef](#)]
3. Chislock, M.F.; Doster, E.; Zitomer, R.A.; Wilson, A.E. *Eutrophication: Causes, Consequences, and Controls in Aquatic Ecosystems*; Springer: Dordrecht, The Netherlands; Berlin/Heidelberg, Germany; London, UK; New York, NY, USA, 2013. [[CrossRef](#)]
4. Hamilton, D.P.; Salmaso, N.; Paerl, H.W. Mitigating harmful cyanobacterial blooms: Strategies for control of nitrogen and phosphorus loads. *Aquat. Ecol.* **2016**, *50*, 351–366. [[CrossRef](#)]
5. Culbertson, A.M.; Martin, J.F.; Aloysius, N.; Ludsin, S.A. Anticipated impacts of climate change on 21st century Maumee River discharge and nutrient loads. *J. Great Lakes Res.* **2016**, *42*, 1332–1342. [[CrossRef](#)]
6. Iavorivska, L.; Veith, T.L.; Cibin, R.; Preisendanz, H.E.; Steinman, A.D. Mitigating lake eutrophication through stakeholder-driven hydrologic modeling of agricultural conservation practices: A case study of Lake Macatawa, Michigan. *J. Great Lakes Res.* **2021**, *47*, 1710–1725. [[CrossRef](#)]

7. Molder, B.; Cockburn, J.; Berg, A.; Lindsay, J.; Woodrow, K. Sediment-assisted nutrient transfer from a small, no-till, tile drained watershed in Southwestern Ontario, Canada. *Agric. Water Manag.* **2015**, *152*, 31–40. [[CrossRef](#)]
8. Rankinen, K.; Keinänen, H.; Bernal, J.E.C. Influence of climate and land use changes on nutrient fluxes from Finnish rivers to the Baltic Sea. *Agric. Ecosyst. Environ.* **2016**, *216*, 100–115. [[CrossRef](#)]
9. Xue, J.; Wang, Q.; Zhang, M. A review of non-point source water pollution modeling for the urban–rural transitional areas of China: Research status and prospect. *Sci. Total Environ.* **2022**, *826*, 154146. [[CrossRef](#)]
10. Hua, L.; Li, W.; Zhai, L.; Yen, H.; Lei, Q.; Liu, H.; Ren, T.; Xia, Y.; Zhang, F.; Fan, X. An innovative approach to identifying agricultural pollution sources and loads by using nutrient export coefficients in watershed modeling. *J. Hydrol.* **2019**, *571*, 322–331. [[CrossRef](#)]
11. Ouyang, W.; Song, K.; Wang, X.; Hao, F. Non-point source pollution dynamics under long-term agricultural development and relationship with landscape dynamics. *Ecol. Indic.* **2014**, *45*, 579–589. [[CrossRef](#)]
12. Zeng, F.; Zuo, Z.; Mo, J.; Chen, C.; Yang, X.; Wang, J.; Wang, Y.; Zhao, Z.; Chen, T.; Li, Y.; et al. Runoff Losses in Nitrogen and Phosphorus From Paddy and Maize Cropping Systems: A Field Study in Dongjiang Basin, South China. *Front. Plant Sci.* **2021**, *12*, 1593. [[CrossRef](#)] [[PubMed](#)]
13. De Filippis, G.; Ercoli, L.; Rossetto, R. A Spatially Distributed, Physically-Based Modeling Approach for Estimating Agricultural Nitrate Leaching to Groundwater. *Hydrology* **2021**, *8*, 8. [[CrossRef](#)]
14. Liu, Y.; Jiang, Q.; Liang, Z.; Wu, Z.; Liu, X.; Feng, Q.; Zou, R.; Guo, H. Lake eutrophication responses modeling and watershed management optimization algorithm: A review. *J. Lake Sci.* **2021**, *33*, 49–63.
15. Wang, Q.; Liu, R.; Men, C.; Guo, L.; Miao, Y. Effects of dynamic land use inputs on improvement of SWAT model performance and uncertainty analysis of outputs. *J. Hydrol.* **2018**, *563*, 874–886. [[CrossRef](#)]
16. Guo, Y.; Wang, X.; Melching, C.; Nan, Z. Identification method and application of critical load contribution areas based on river retention effect. *J. Environ. Manag.* **2021**, *305*, 114314. [[CrossRef](#)]
17. Zheng, J.; Li, W.; Huo, S.; He, Z.; Cao, X.; Ma, C.; Huang, W. Application and Development Trend of SPARROW Model in Water Environment management. *Res. Environ. Sci.* **2021**, *34*, 2200–2207.
18. Ouyang, W.; Wei, P.; Gao, X.; Srinivasan, R.; Yen, H.; Xie, X.; Liu, L.; Liu, H. Optimization of SWAT-Paddy for modeling hydrology and diffuse pollution of large rice paddy fields. *Environ. Model. Softw.* **2020**, *130*, 104736. [[CrossRef](#)]
19. Kast, J.B.; Apostel, A.M.; Kalcic, M.M.; Muenich, R.L.; Dagnew, A.; Long, C.M.; Evenson, G.; Martin, J.F. Source contribution to phosphorus loads from the Maumee River watershed to Lake Erie. *J. Environ. Manag.* **2020**, *279*, 111803. [[CrossRef](#)]
20. Panagopoulos, Y.; Makropoulos, C.; Baltas, E.; Mimikou, M. SWAT parameterization for the identification of critical diffuse pollution source areas under data limitations. *Ecol. Model.* **2011**, *222*, 3500–3512. [[CrossRef](#)]
21. Pulighe, G.; Bonati, G.; Colangeli, M.; Traverso, L.; Lupia, F.; Altobelli, F.; Marta, A.D.; Napoli, M. Predicting Streamflow and Nutrient Loadings in a Semi-Arid Mediterranean Watershed with Ephemeral Streams Using the SWAT Model. *Agronomy* **2019**, *10*, 2. [[CrossRef](#)]
22. Shen, Z.; Qiu, J.; Hong, Q.; Chen, L. Simulation of spatial and temporal distributions of non-point source pollution load in the Three Gorges Reservoir Region. *Sci. Total Environ.* **2014**, *493*, 138–146. [[CrossRef](#)] [[PubMed](#)]
23. Zhang, X.; Chen, X.; Zhang, W.; Peng, H.; Xu, G.; Zhao, Y.; Shen, Z. Impact of Land Use Changes on the Surface Runoff and Nutrient Load in the Three Gorges Reservoir Area, China. *Sustainability* **2022**, *14*, 2023. [[CrossRef](#)]
24. Li, Y.; Wang, F.; Yan, W.; Lv, S.; Li, Q.; Yu, Q.; Wang, J. Enhanced nitrogen imbalances in agroecosystems driven by changing cropping systems in a coastal area of eastern China: From field to watershed scale. *Environ. Sci. Process. Impacts* **2019**, *21*, 1532–1548. [[CrossRef](#)] [[PubMed](#)]
25. Wang, J.; Lu, J.; Zhang, Z.; Han, X.; Zhang, C.; Chen, X. Agricultural non-point sources and their effects on chlorophyll-a in a eutrophic lake over three decades (1985–2020). *Environ. Sci. Pollut. Res.* **2022**, *29*, 46634–46648. [[CrossRef](#)] [[PubMed](#)]
26. Ji, N.; Liu, Y.; Wang, S. The sources characteristics of stable isotope organic carbon and nitrogen in suspended particles and surface sediments in Lake Erhai and their water quality implications. *Hupo Kexue* **2022**, *34*, 118–133.
27. *Analysis Report on the Temporal and Spatial Dynamic Change of the Total Amount of Pollution Entering the Lake of Erhai Basin*, Yunnan Research Academy of Eco-Environmental Sciences & Chinese Research Academy of Environmental Sciences: Kunming, China, 2021.
28. Wang, S.; Guo, S.; Zhai, L.; Hua, L.; Khoshnevisan, B.; Wang, H.; Liu, H. Comprehensive effects of integrated management on reducing nitrogen and phosphorus loss under legume-rice rotations. *J. Clean. Prod.* **2022**, *361*, 132031. [[CrossRef](#)]
29. Huang, H.; Wang, Y.; Li, Q. Climatic Characteristics over Erhai Lake Basin in the Late 50 Years and the Impact on Water Resources of Erhai Lake. *Meteorol. Mon.* **2013**, *39*, 436–442.
30. Li, Y.; Liu, H.B.; Lei, Q.L.; Hu, W.L.; Wang, H.Y.; Zhai, L.M.; Ren, T.Z.; Lian, H.S. Impact of human activities on Net anthropogenic Nitrogen Inputs (NANI) at Township scale in Erhai Lake Basin. *Environ. Sci.* **2018**, *39*, 4189–4198.
31. Ma, W.; Jiang, R.; Zhou, Y.; Su, J.; Xin, L. Study on diagnosis of water environmental problems and water quality protection countermeasures in Erhai Lake Basin. *Yangtze River* **2021**, *52*, 45–53.
32. Jin, C. *Study on Non-Point Source Pollution in the Western and Northern Regions of Erhai Basin Using SWAT Model*; Chinese Research Academy of Environmental Sciences: Beijing, China, 2018.
33. Shang, X.; Wang, X.; Zhang, D.; Chen, W.; Chen, X.; Kong, H. An improved SWAT-based computational framework for identifying critical source areas for agricultural pollution at the lake basin scale. *Ecol. Model.* **2011**, *226*, 1–10. [[CrossRef](#)]

34. Geospatial Data Cloud Site, Computer Network Information Center, Chinese Academy of Sciences. 2018. Available online: <http://www.gscloud.cn/> (accessed on 20 October 2018).
35. Soil Science Database. Available online: <https://vdb3.soil.csdb.cn/> (accessed on 20 October 2018).
36. China Meteorological Data Sharing Service System. Available online: <http://data.cma.cn/> (accessed on 20 October 2018).
37. Li, W.; Zhai, L.; Lei, Q.; Wollheim, W.M.; Liu, J.; Liu, H.; Hu, W.; Ren, T.; Wang, H.; Liu, S. Influences of agricultural land use composition and distribution on nitrogen export from a subtropical watershed in China. *Sci. Total Environ.* **2018**, *642*, 21–32. [[CrossRef](#)] [[PubMed](#)]
38. Yu, C.; Chu, J.Y.; Bai, X.H.; Liu, W.L. Seasonal variation of nitrogen and phosphorus in Miju River and Lake Erhai and influencing factors. *Acta Ecol. Sinica* **2011**, *31*, 7104–7111.
39. Xiang, S.; Wu, Y.; Lv, X.J.; Gao, S.J.; Chu, Z.S.; Pang, Y. Characteristics and Spatial Distribution of Agricultural Non-Point Source Pollution in Erhai Lake Basin and Its Classified Control Strategy. *Res. Environ. Sci.* **2020**, *33*, 2474–2483.
40. Li, H.; Liu, J.; Li, G.; Shen, J.; Bergström, L.; Zhang, F. Past, present, and future use of phosphorus in Chinese agriculture and its influence on phosphorus losses. *Ambio* **2015**, *44*, 274–285. [[CrossRef](#)]
41. Binghui, Z.; Jing, C.; Kun, W.; Zhaosheng, C.; Xia, J. Theoretical basis and Chinese practice for environmental protection of lakes with better water quality. *J. Lake Sci.* **2022**, *34*, 699–710. [[CrossRef](#)]
42. Scheffer, M.; Donk, E. Multiplicity of stable states in freshwater systems. In *Bio-manipulation Tool for Water Management, Proceedings of an International Conference Held in Amsterdam, The Netherlands, 8–11 August, 1989*; Springer: Dordrecht, The Netherlands, 1990; pp. 475–486. [[CrossRef](#)]
43. Scheffer, M.; Carpenter, S.; Foley, J.A.; Folke, C.; Walker, B. Catastrophic shifts in ecosystems. *Nature* **2001**, *413*, 591–596. [[CrossRef](#)]
44. Gao, W.; Duan, Z.; Yan, C.; Liu, C. Influence of nutrient mitigation measures on the fractional export of watershed inputs in an urban watershed. *Environ. Sci. Pollut. Res.* **2020**, *27*, 18521–18529. [[CrossRef](#)]
45. Yang, X.; Zhu, Z.; Zhang, J.; Li, S. Temporal and spatial distribution of nitrogen and phosphorus in inflow rivers of Fuxian Lake. *J. Tianjin Norm. Univ. Nat. Sci. Ed.* **2020**, *40*, 37–43.
46. Wang, M.; Stokal, M.; Burek, P.; Kroeze, C.; Ma, L.; Janssen, A.B. Excess nutrient loads to Lake Taihu: Opportunities for nutrient reduction. *Sci. Total Environ.* **2019**, *664*, 865–873. [[CrossRef](#)]
47. Wu, H.; Yang, T.; Liu, X.; Li, H.; Gao, L.; Yang, J.; Li, X.; Zhang, L.; Jiang, S. Towards an integrated nutrient management in crop species to improve nitrogen and phosphorus use efficiencies of Chaohu Watershed. *J. Clean. Prod.* **2020**, *272*, 122765. [[CrossRef](#)]
48. Wang, L.J.; Tian, Z.B.; Li, Y.J.; Chen, J.X.; Li, L.Q.; Wang, X.; Zhao, Y.M.; Zheng, B.H. Trend and Driving Factors of Water Environment Change in Dongting Lake in the Last 30 Years. *Res. Environ. Sci.* **2020**, *33*, 1140–1149.
49. Li, P.; Zheng, B.; Liu, C.; Zhou, W.; Yu, J.; Liu, Y. Prediction on pollution contribution of N and P from agricultural non-point source pollution in Poyang Lake watershed. In *Proceedings of the 2011 International Conference on Remote Sensing, Environment and Transportation Engineering, Nanjing, China, 24–26 June 2011*.
50. Xiang, R.; Wang, L.; Li, H.; Tian, Z.; Zheng, B. Water quality variation in tributaries of the Three Gorges Reservoir from 2000 to 2015. *Water Res.* **2021**, *195*, 116993. [[CrossRef](#)] [[PubMed](#)]
51. Russo, T.A.; Tully, K.; Palm, C.; Neill, C. Leaching losses from Kenyan maize cropland receiving different rates of nitrogen fertilizer. *Nutr. Cycl. Agroecosyst.* **2017**, *108*, 195–209. [[CrossRef](#)] [[PubMed](#)]
52. He, W.; Jiang, R.; He, P.; Yang, J.; Zhou, W.; Ma, J.; Liu, Y. Estimating soil nitrogen balance at regional scale in China’s croplands from 1984 to 2014. *Agric. Syst.* **2018**, *167*, 125–135. [[CrossRef](#)]
53. Chen, L.; Li, J.; Xu, J.; Liu, G.; Wang, W.; Jiang, J.; Shen, Z. New framework for nonpoint source pollution management based on downscaling priority management areas. *J. Hydrol.* **2022**, *606*, 127433. [[CrossRef](#)]
54. Epelde, A.M.; Antiguada, I.; Brito, D.; Jauch, E.; Neves, R.; Garneau, C.; Sauvage, S.; Sánchez-Pérez, J.M. Different modelling approaches to evaluate nitrogen transport and turnover at the watershed scale. *J. Hydrol.* **2016**, *539*, 478–494. [[CrossRef](#)]
55. Ferrant, S.; Oehler, F.; Durand, P.; Ruiz, L.; Salmon-Monviola, J.; Justes, E.; Dugast, P.; Probst, A.; Probst, J.-L.; Perez, J.M.S. Understanding nitrogen transfer dynamics in a small agricultural catchment: Comparison of a distributed (TNT2) and a semi distributed (SWAT) modeling approaches. *J. Hydrol.* **2011**, *406*, 1–15. [[CrossRef](#)]
56. Li, W.; Lei, Q.; Yen, H.; Zhai, L.; Hu, W.; Li, Y.; Wang, H.; Ren, T.; Liu, H. Investigation of watershed nutrient export affected by extreme events and the corresponding sampling frequency. *J. Environ. Manag.* **2019**, *250*, 109477. [[CrossRef](#)]